12 Phase transitions and superconducting photon detectors

H. Grundmann, O. Bossen, K. Inderbitzin, M. Reibelt, H. Bartolf, S. Siegrist, L. Gómez (visiting scientist), A. Engel and A. Schilling

in collaboration with:
Paul Scherrer Institute, University of Bern (K. Krämer), EPF Lausanne (H. Berger), Bhaba Atomic Research Center (G. Ravikumar), Tohoku University (N. Toyota), Universität Karlsruhe (K. Il'in), Deutsches Zentrum für Luft- und Raumfahrt (H.-W. Hübers, A. Semenov), FIRST Lab ETH Zürich.

12.1 Physics of superconducting thin-film nanostructures and fast single-photon detectors

In recent years we have developed a nanostructuring process that allows us to produce superconducting planar structures in the sub-100 nm range (1). Using this process we have fabricated state-of-the-art superconducting nanowire single-photon detectors (SNPD) with quantum-efficiencies in the percent range and pulse widths of only a few nanoseconds with rise times of ~ 200 ps, see Fig. 12.1. These kinds of detectors receive growing interest in the field of quantum information applications (2) and other areas of research and technology, where speed and fast response times are crucial. The working principle of the detector can be sketched in the following way: A superconducting wire of small cross-section—typical dimensions are 100 nm width and 5 nm thickness—is held at a temperature, T, well below its superconducting transition temperature ($T \approx 0.5T_c$). It is operated by applying a bias current, I_b, very close to the critical current (typically I_b between 90% and 95% of I_c). Then, the absorption of a photon constitutes a sufficient disturbance to temporarily drive a section of the wire into its resistive state, which can be registered as a voltage pulse.

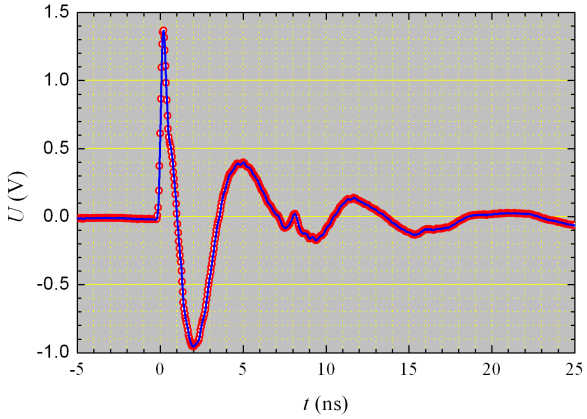

Figure 12.1: Photon-absorption event, indicated by a voltage pulse. The signal was recorded with a digital oscilloscope after amplification of the original pulse. The oscillations after the primary peak at t=0 are due to circuit resonances and reflections.

One important figure of merit is the noise-equivalent power (NEP) of a detector, which is a measure for the probability to detect a "false" photon, when in reality no photon has been absorbed. SNPD have a very low NEP, outperforming most other detector technologies. The NEP of a single-photon detector is proportional to $\sqrt{\Gamma_{\mathrm{DC}}}$, where Γ_{DC} is the dark-count rate of the detector, *i.e.* the number of events per second without the absorption of a real photon. We have measured the dark counts for three detectors with different strip widths as a function of the reduced bias current, as shown in Fig. 12.2. In an attempt to describe the nearly exponential dependence on the bias current we have developed three models based on three different fluctuation mechanisms (3).

One possible fluctuation mechanism is based on so called thermally-activated phase slips (TAPS) as they appear in one-dimensional superconducting wires (4), resulting in a non-

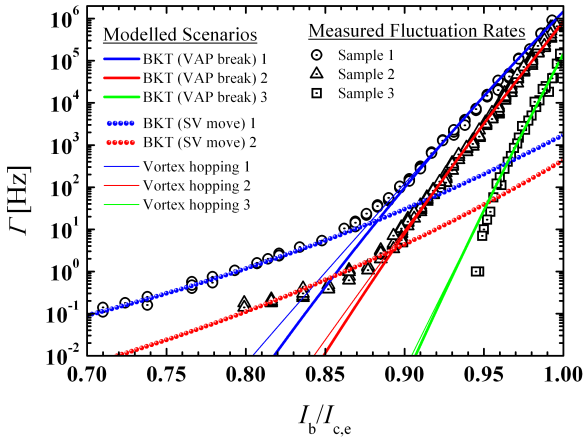

Figure 12.2: Dark count rates as a function of reduced bias current I_b/I_c with widths w=53, 83 and 171 nm for samples 1, 2 and 3, respectively. The symbols mark the experimental dark-count rates. The colored lines represent the calculated rates based on the BKT model (bold and dotted lines), and the vortex hopping model (thin lines). For the 170 nm wide meander the SV BKT mechanism may be below our detection limit.

vanishing resistance even below T_c. However, taking into account the effective cross-sectional area of our meander strips, we were not able to consistently describe the dark-count rates based on TAPS events. This is most likely due to the fact that the cross-sectional area of even the narrowest strip is still about 12 times the coherence length squared, which is usually taken as a criterion for one-dimensionality.

Supported by independent analyses of resistance *versus* temperature measurements near T_c we therefore assume the meanders to be still in the two-dimensional limit (5). Analogous to TAPS in one dimensions, magnetic vortices in two dimensions can be elementary, thermally-activated excitations. We considered two different vortex excitations. First, vortex-antivortex pairs (VAP) of a Berezinskii-Kosterlitz-Thouless (BKT) type (6) that become thermally unbound due to the applied bias current and lead to dark-count events. The other mechanism is based on single vortices hopping over edge barriers that are always present in finite-size superconducting films (7). Both vortex models are able to consistently describe the experimentally measured dark-count rates. The vortex-antivortex model may even allow to describe a "tail" observed for low bias currents (see Fig. 12.2), taking into account that in narrow superconducting strips, single unbound vortices will always be present. However, at the current stage we can also not exclude experimental artifacts (*e.g.* electro-magnetic interferences, ripples in the bias-current, etc.) as the cause for the observed "tail" for low bias currents.

12.2 Unveiling the peak effect in resistivity data of Nb_3Sn using vortex shaking

One of the important goals of our investigations in the field of vortex physics in type-II superconductors is to clarify the influence of transverse or longitudinal "vortex shaking" by the application of an oscillating magnetic field on the physical quantities. To obtain a complete physical picture we have studied possible related effects on the electrical resistivity, a quantity that is known to crucially depend on the details of the vortex physics, in particular of vortex pinning. We have observed (to the best of our knowledge for the first time) that the so-called peak effect in the resistivity data near the upper-critical field of a type-II superconductor can be "switched on and off" by the application of such an external oscillating magnetic field h_{ac} parallel to the main magnetic field H (8).

These experiments have been done on a Nb_3Sn single crystal (in collaboration with N. Toyota, Tohoku University, Sendai, Japan) using a home-built resistivity probe equipped with an ac "shaking" coil that can be used in a commercial PPMS (Physical Property Measurement System, Quantum Design, see Fig. 12.3). In Fig. 12.4 we show the manifes-

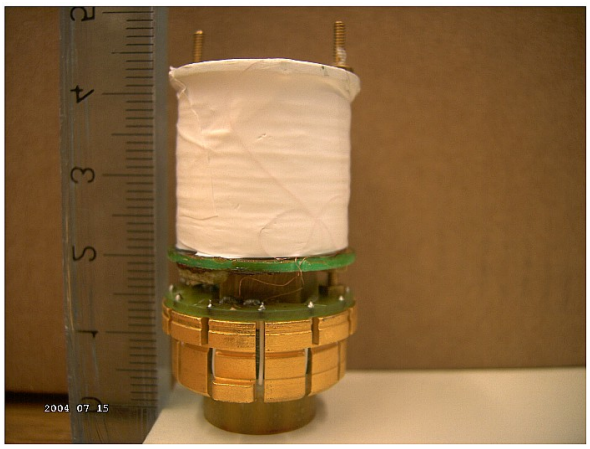

Figure 12.3: Resistivity "puck" with a coil mounted to apply an ac "shaking" magnetic field.

tation of the peak effect as we have measured it conventionally by dc magnetization-hysteresis loop measurements. In Fig. 12.5 we show the temperature dependence of the resistance of the same sample for different magnetic fields H. While the data in the upper part of Fig. 12.5 were taken without any oscillating magnetic field h_{ac}, the data displayed in the lower part were measured with $\mu_0 h_{ac} = 0.58$ mT$\parallel H$ at a frequency $f = 1$ kHz. With $h_{ac} = 0$, no feature other than the sharp transition to superconductivity is discernible. With an additional small oscillating magnetic field, however, a clear signature due to the peak effect appears for $\mu_0 H \leq 3$ T. This signature consists

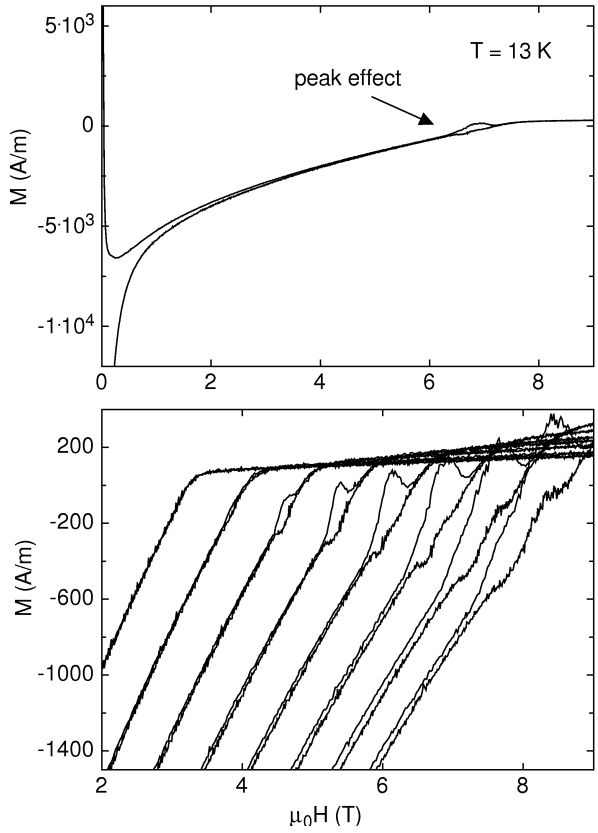

Figure 12.4: Upper panel: dc magnetization-hysteresis curve of a Nb_3Sn single crystal for T = 13 K. Lower panel: parts of the dc magnetization hysteresis curves for different temperatures (from left to right): 15.5 K, 15 K, 14.5 K, 14 K, 13.5 K, 13 K, 12.5 K, 12 K.

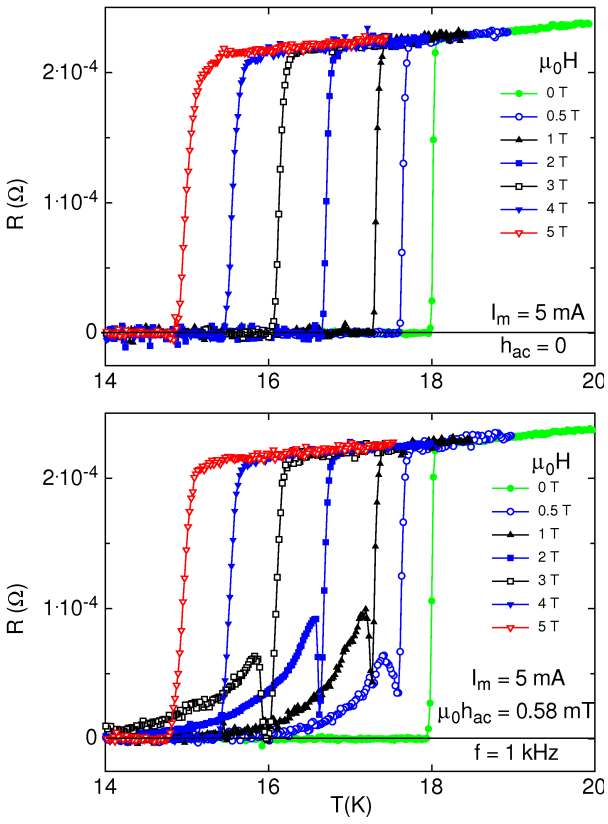

Figure 12.5: Resistance R(T) for magnetic fields $H \parallel c$ without (upper panel) and with (lower panel) an oscillating "shaking" magnetic field (f = 1 kHz, $\mu_0 h_{ac} = 0.58$ mT) superimposed.

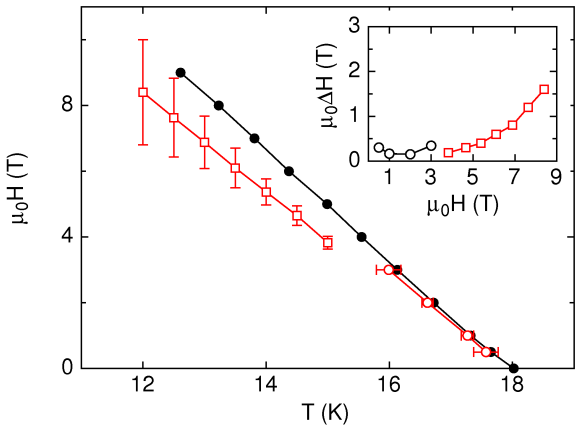

Figure 12.6:
Magnetic phase diagram of the investigated Nb_3Sn single crystal as derived from the data shown in Fig. 12.4 and 12.5. Filled circles: upper critical field. Open circles: peak-effect region from R(T) measurements with "vortex shaking". Open squares: peak-effect region from M(H) data. Inset: Magnetic-field dependence of the width of the peak-effect region $\mu_0\Delta H$ (Circles: resistivity; squares: dc magnetization).

of a region with finite resistance for temperatures T well below T_c which we attribute to the dissipative motion of magnetic vortices, and a pronounced drop right below T_c that must indicate enhanced flux pinning in the peak-effect region.

We have systematically studied the dependence of this effect on the transport current, the "shaking" frequency f and the amplitude h_{ac} of the oscillating magnetic field. The resulting magnetic phase diagram shown in Fig. 12.6 clearly illustrates the 1:1 correspondence of the magnetically and the resistively determined peak-effect data.

We conclude that this technique of measuring $R(T)$ with an external, continuously oscillating magnetic field may be even more sensitive to explore the peak effect than inferring it from corresponding magnetization $M(H)$ measurements alone, at least in some parts of the magnetic phase diagram of a sample. While the peak-effect feature is not discernible at temperatures higher than 15 K in the $M(H)$ data shown in Figs. 12.4 and 12.5, the resistivity data (taken in combination with an ac magnetic field) reveal the peak-effect region also in this high-temperature region of the magnetic phase diagram. Therefore we believe that such resistivity measurements, in combination with an oscillating magnetic field, may turn out to be a versatile tool not only for the investigation of the peak effect, but also for studying other effects where the pinning of magnetic flux lines plays a certain role.

12.3 Construction of an ac-calorimetry experiment for vortex-shaking experiments

In the past we have done numerous experiments using differential-thermoanalysis (DTA) techniques to study phase transitions of various superconductors. Our recent calorimetric experiments on the above mentioned Nb_3Sn single crystal using an external oscillating magnetic field (not shown here) demonstrated, however, that self-heating effects due to eddy currents in combination with a finite resistance near T_c (or as a result of a sudden dissipative motion of vortices) are in some cases limiting the applicability of this technique. To overcome this obstacle and to obtain an even higher resolution in the vicinity of a possible sharp phase transition, we decided to build a specific-heat experiment based on ac calorimetry techniques that uses a periodic heating of the sample and allows for the use of lock-in amplifier electronics. As the base temperature of a sample can be fixed even with self-heating effects present, this technique should allow for much more accurate investigations of possible vortex phase transitions near the upper-critical field of type-II superconductors and in combination with an external ac "shaking" magnetic field.

Figure 12.7: Ac calorimeter puck that fits into a commercial PPMS (Quantum Design Inc.) system.

Two prototypes of such an experiment have been constructed. In both cases a thin sapphire disc suspended on nylon fibers acts as a sample platform, and the sample heater consists of a miniature thick-film resistor. In one version, the temperature difference to the thermal bath is measured with a thermopile of 30 gold-iron *vs.* chromel thermocouples connected in series. In a second version, this difference is measured with resistive thermometers in a Wheatstone-like differential configuration (see Fig. 12.7). Both setups are designed to fit into a commercial PPMS system that also provides the main magnetic field and the base temperature of the thermal bath. This will allow for a fast data acquisition and a reliable operation from $T = 1.8$ K up to room temperature.

12.4 Structural phase transition in magnetic insulators

There has been considerable interest in the unique properties of quantum-spin systems over the last decade. Much effort has been taken, experimentally as well as theoretically, to understand their behaviour in a magnetic field. A certain class of phase transitions, occurring at a critical field H_c and at low temperatures, has been interpreted in terms of a Bose-Einstein condensation (BEC) of magnetic quasi-particles (9; 10).

Previous work in our group focused on the three-dimensional spin system $TlCuCl_3$, mainly because its critical field ($\mu_0 H_c \approx 5.5$ T (12)) is well within reach of our existing cryo-system.

To prove whether a true BEC of the magnetic quasi-particles is formed or not, we earlier attempted to excite collective modes of the spin system via ac susceptometry, but no sign of a long-lived collective mode could be found (13).

We have then proposed that the symmetry of the spin in dimerized quantum magnets spontaneously changes as soon as the BEC sets in (14). The distortion of axial symmetry fixes the phase of the condensate to a constant value and therefore prevents the system from becoming a true superfluid. Signs for such a lattice distortion have been previously reported (15), but the corresponding changes in the crystal lattice could not be assigned to specific atoms in the unit cell of $TlCuCl_3$.

To investigate if a distortion of the axial symmetry takes place at the BEC, we decided to carry out diffraction experiments on a $TlCuCl_3$ single-crystal using both neutron- (at PSI Villigen) and synchrotron x-ray scattering (at the ESRF in Grenoble) techniques. The experiments will be carried out in high magnetic fields ($\mu_0 H = 10$ T) and at low temperature ($T = 1.9$ K).

The single crystals needed for these experiments are grown by Dr. Karl Krämer, University of Bern.

[1] H. Bartolf, A. Engel, L. Gómez, and A. Schilling, Raith application note, Physics Institute of the University of Zurich, Switzerland (2008).

[2] R. H. Hadfield, Nature Photonics, **3**, (2009) 696.

[3] H. Bartolf, A. Engel, A. Schilling, K. Il'in, M. Siegel, H.-W. Hübers, and A. Semenov, Phys. Rev. B, **81**, (2010) 024502.

[4] K. Y. Arutyunov, D. S. Golubev, and A. D. Zaikin, Phys. Rep., **464**, (2008) 1.

[5] A. Engel, H. Bartolf, A. Schilling, A. Semenov, H.-W. Hübers, K. Il'in, and M. Siegel, J. Mod. Optics, **56**, (2009) 352.

[6] J. M. Kosterlitz and D. J. Thouless, J. Phys. C, **6**, (1973) 1181.

[7] J. R. Clem, Bull. Am. Phys. Soc., volume 43 (1998), 411.

[8] M. Reibelt et al., Phys. Rev. B., **81** (2010) 094510.

[9] T. Giamarchi, A. M. Tsvelik, Phys. Rev. B, **59**, (1999) 11398.

[10] I. Affleck, Phys. Rev. B, **43**, (1991) 3215.

[11] H. Tanaka et al., J. Phys. Soc. Jap., **70**, (2001) 939.

[12] T. Nikuni et al., Phys. Rev. Lett., **84**, (2000) 5868.

[13] R. Dell'Amore, doctoral thesis, University of Zurich, 2008.

[14] R. Dell'Amore, A. Schilling and K. Krämer, Phys. Rev. B, **79**, (2009) 014438.

[15] O. Vyaselev et al., Phys. Rev. Lett., **92**, (2004) 207202.